

FTIR Spectroscopy

AUTHORS

Aswathy Balakrishnan^{1,3}, Caio H. N. Barros¹
Elizabeth Topp^{1,2}

¹ *Formulation and Stability Laboratory
NIBRT – National Institute for Bioprocessing
Research and Training
Foster Avenue, Mount Merrion
Blackrock, Dublin, Ireland*

² *Department of Industrial and Physical Pharmacy
College of Pharmacy, Purdue University
West Lafayette, Indiana 47907-2091
United States*

³ *School of Chemical and Bioprocess Engineering,
University College Dublin (UCD), Belfield, D04 V1W8,
Dublin, Ireland*

Effects of Ionizable and Non-ionizable Excipients on Lyophilized RNA Formulations Using FTIR-ATR Technology

Introduction

The COVID-19 pandemic brought mRNA messenger ribonucleic acid vaccines into international prominence. mRNA is highly unstable

and storage and/or transportation of these vaccines at -80 °C has been required to avoid degradation. There are ongoing attempts to improve the storage stability of mRNA vaccines by converting them to solid forms using various drying methods. Lyophilization is one such method and has the potential to stabilize mRNA, but there are few reports that describe the interactions of lyophilized mRNA with excipients (e.g., sugars, salts, and lipids) in the solid state.¹ Methods such as capillary electrophoresis, mass spectrometry, and reversed phase HPLC, among others, are currently used to analyze mRNA. However, these methods require reconstitution and samples cannot be analyzed directly in solid state form.² In this application note, the PerkinElmer Spectrum Two™ FTIR Spectrometer with attenuated total reflectance accessory (ATR-FTIR) was used to probe the interactions of RNA with various excipients in lyophilized solid samples. The results demonstrate the ability of the instrument to detect RNA peaks of interest and to carry out post-processing of the spectra. RNA band positions were sensitive to excipient type and RNA: excipient ratio, suggesting utility of the method in developing stable solid mRNA formulations.

Materials

Analyses were carried out using a PerkinElmer Spectrum Two FTIR Spectrometer coupled with an Attenuated Total Reflectance accessory. Here, RNA from the yeast *Saccharomyces cerevisiae* (average of 100 nt) is used as a simple and affordable model system for mRNA. Yeast RNA (Roche-10109223001) and sodium chloride (ACS Reagent Grade, >99.0%) were purchased from Sigma-Aldrich. Sucrose (Alfa Aesar, ultrapure, 99%) and 1,2-dioleoyloxy-3-(trimethylammonium)propane (DOTAP) chloride (Selleck Chemicals) were purchased from Thermo Fisher Scientific. Lyophilization was performed in a Telstar LyoBeta 3PS freeze-dryer as described below.

Methods

Solutions of yeast RNA (1 mg/mL) were prepared with sucrose and sodium chloride excipients at three different ratios (RNA: Excipient = 1:2, 1:1 and 2:1). Cationic lipid formulations were prepared by adding DOTAP chloride (1 mg/mL in 1% EtOH) to these solutions in two different ratios (DOTAP: RNA: Excipient = 1:2:2 and 1:1:1). 1 mL of each solution was then added to 2 mL glass vials for lyophilization, a total of 10 vials. A control vial containing only RNA (1 mg/mL) was also prepared. The lyophilization cycle consisted of freezing at -40 °C for six hours, primary drying at -35 °C for 26 hours at a pressure of 0.130 mbar, and secondary drying at 25 °C for eight hours at the lowest pressure that the instrument can attain.

The lyophilized samples were immediately frozen at -20 °C prior to analysis to minimize degradation. After thawing, ATR-FTIR was carried out on each sample with 64 scans and at a resolution of 2 cm⁻¹. The baselines of the spectra were corrected, and spectra were normalized to account for the deviations in sample amount. Denaturing gel electrophoresis (agarose 1% in MOPS-formaldehyde buffer) was performed on each sample to confirm the integrity of RNA after lyophilization. FTIR spectra were also obtained for samples of RNA: NaCl = 1:1 at pre-lyophilization pH of 3, 5, 6 and 9.5, with 64 scans at a resolution of 4 cm⁻¹. Figure 1 shows a flowchart of the workflow.

Results and Discussion

The FTIR spectrum of lyophilized RNA without excipient shows three bands of interest (Fig. 2A). Based on previous reports,^{3,4} the band near 1048 cm⁻¹ is assigned to C-O stretching of the ribose sugar, the band near 1215 cm⁻¹ is assigned to antisymmetric stretching of the phosphate and is characteristic of the phosphodiester backbone of a nucleic acid, and the band near 1683 cm⁻¹ is assigned to stretching of nucleobase carbonyl groups.

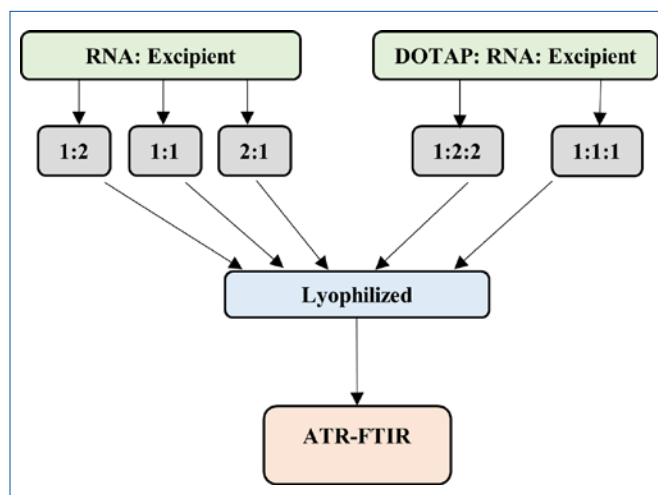


Figure 1: Flowchart of methods used for ATR-FTIR studies of yeast RNA with sucrose and NaCl excipients.

The positions of the bands shifted when RNA was co-lyophilized with sucrose or NaCl (Fig. 2B, C, D), suggesting interactions between the excipients and RNA in the solid state:

C-O Stretching Band - The RNA C-O band in samples containing sucrose shifted to lower wavenumber by as much as 5 cm⁻¹ (Fig. 2B, D), suggesting interactions between sucrose and ribose, though overlapping signal from sucrose hydroxyl groups may interfere. Smaller shifts of the C-O band to lower wavenumber were observed in samples containing NaCl (Fig. 2C, D) and did not trend with RNA: NaCl ratio.

Phosphate Band - The RNA phosphate band for samples containing sucrose shifted to lower wavenumber by approximately 3 cm⁻¹ and was not affected by the RNA: sucrose ratio (Fig. 2B, D). This suggests interactions between the phosphate group of the RNA backbone and sucrose. In samples containing NaCl, the phosphate band shifts towards higher or lower wavenumber, with the direction and extent of the shift affected by the RNA: NaCl ratio. This suggests interaction between sodium chloride and negatively charged phosphate group of the RNA backbone that may be affected by the concentration of Na⁺ ion.

Carbonyl Band - The C=O band position is unaffected by excipient type or RNA: excipient ratio, suggesting that there are no interactions involving the nucleobase carbonyl groups. The C=O band has a number of shoulders, perhaps reflecting differences among the C=O groups of the different nucleobases; individual carbonyl types and their interactions are not resolved.

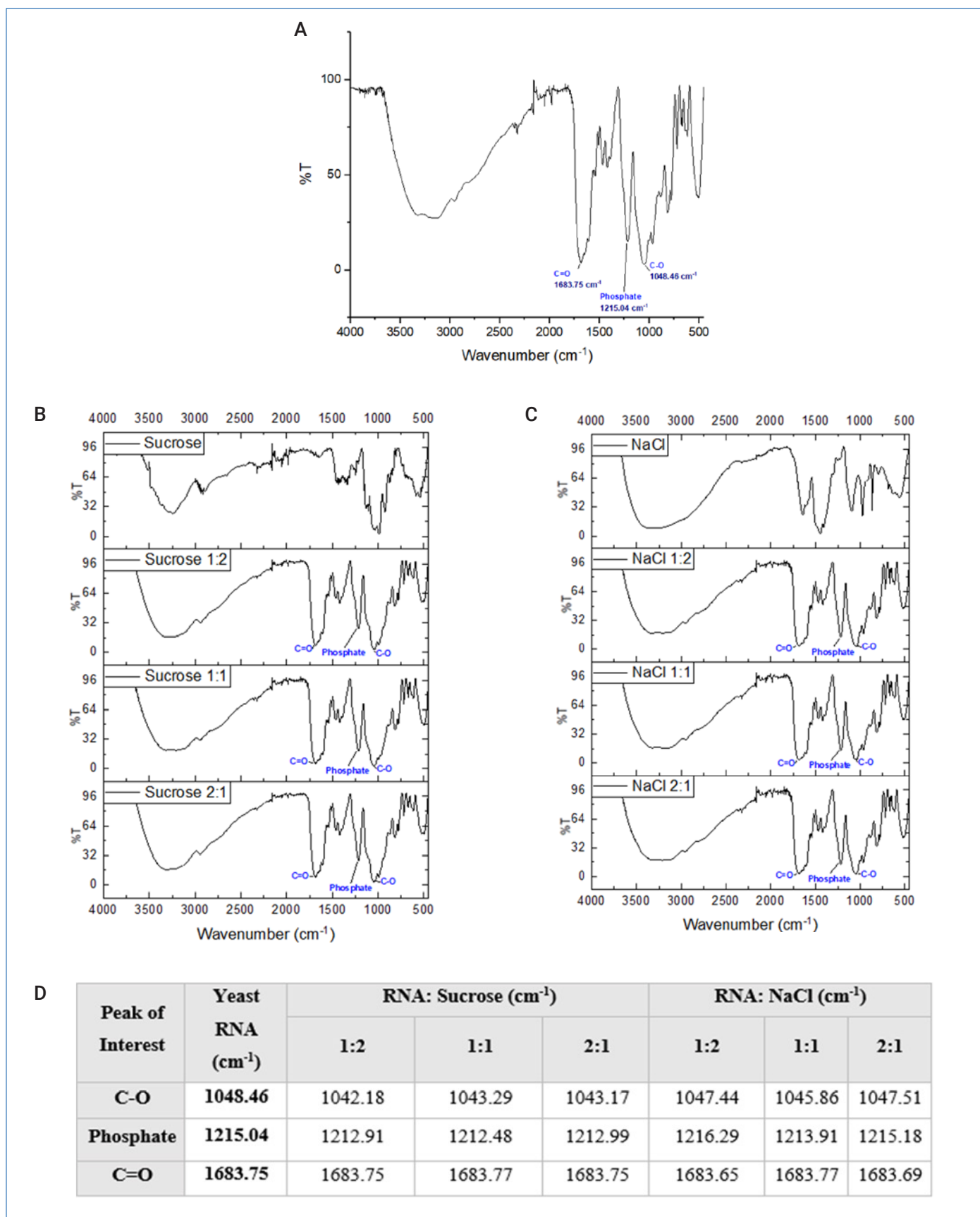


Figure 2: FTIR spectra of lyophilized RNA formulations. (A) Yeast RNA lyophilized without excipient (B) RNA: Sucrose at ratios of 1:0, 1:1, 1:2, 2:1, (C) RNA: NaCl at ratios of 1:0, 1:1, 1:2, 2:1, and (D) Band position of RNA peaks of interest

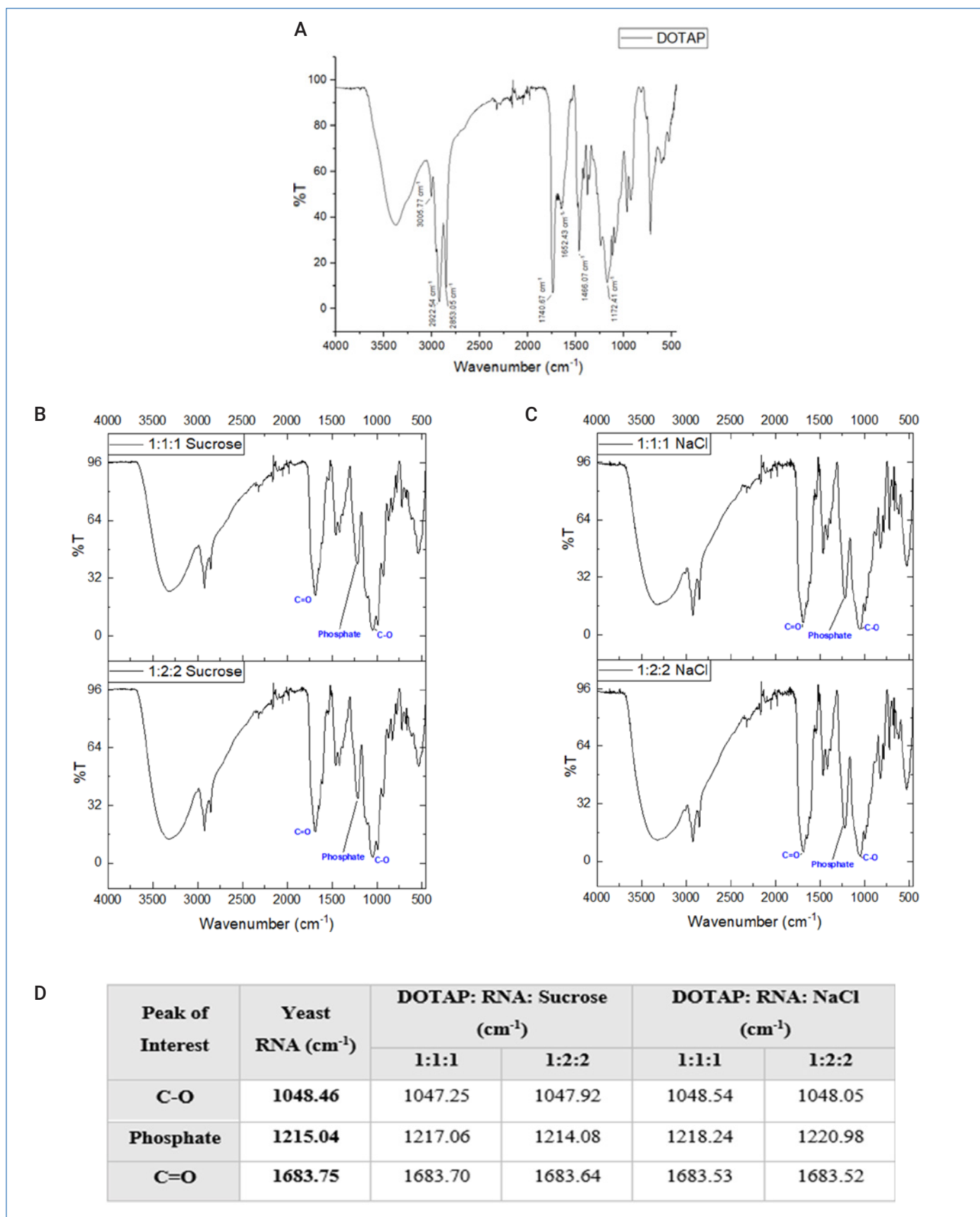


Figure 3: FTIR spectra of RNA formulations. (A) DOTAP Chloride (not lyophilized). (B) DOTAP: RNA: Sucrose at ratios 1:1:1, 1:2:2. (C) DOTAP: RNA: NaCl at ratios 1:1:1, 1:2:2. (D) Band position of RNA peaks of interest.

In RNA vaccines, mRNA is formulated in lipid nanoparticles (LNP) to enable delivery to the cytoplasm. Condensation of anionic mRNA with cationic lipids in these LNP is central to vaccine effectiveness. The effects of the cationic lipid DOTAP on FTIR spectra were evaluated in lyophilized solids containing sucrose or NaCl. With the addition of DOTAP, the C-O and C=O band positions were essentially unchanged from RNA lyophilized without excipient for both sucrose and NaCl containing solids (Fig. 3A, B, C) The phosphate peak shifted towards higher wavenumbers and the magnitude of the shift was affected by excipient type and DOTAP: RNA: excipient ratios (Fig. 4B). This suggests that DOTAP interacts with RNA via phosphate groups even in the presence of ionizable excipient NaCl.

There is no shift in the carbonyl band on addition of DOTAP. However, as the pre-lyophilization pH is increased, there is splitting of this band in RNA: NaCl containing samples (Fig. 5). At pH 3, the main band appears at 1689 cm^{-1} which then splits into two peaks (1682 cm^{-1} and 1651 cm^{-1}) at pH 5. With further pH increases (pH 6, 9.5; Fig. 5), the main band shifts to 1650 cm^{-1} , suggesting different conformations or environments for the nitrogenous bases.⁵

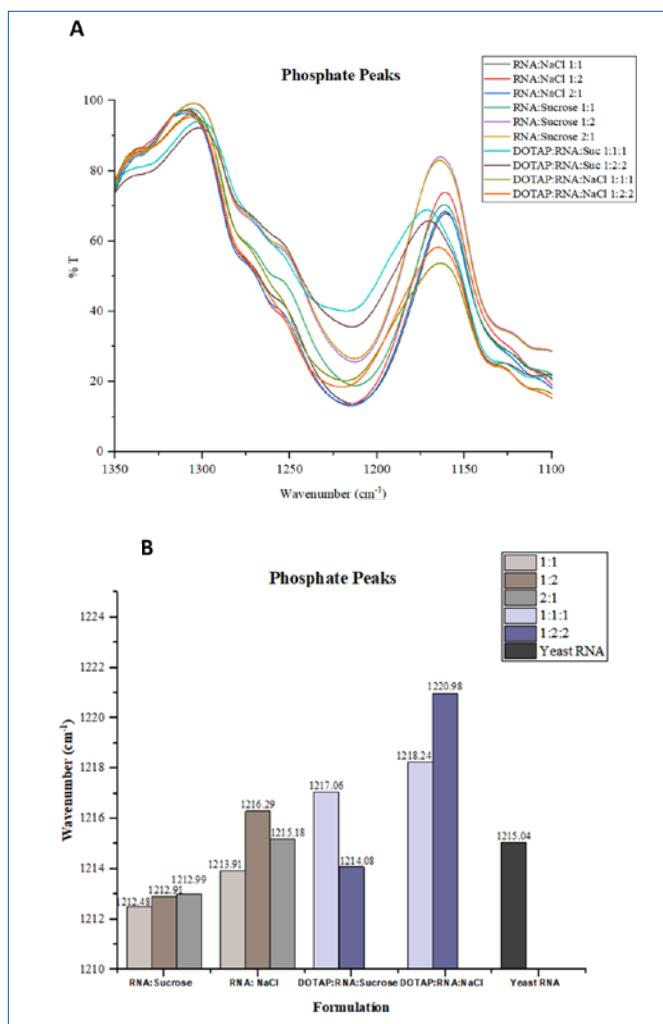


Figure 4: Phosphate peaks of RNA formulations represented as (A) FTIR Spectra (B) Bar graph.

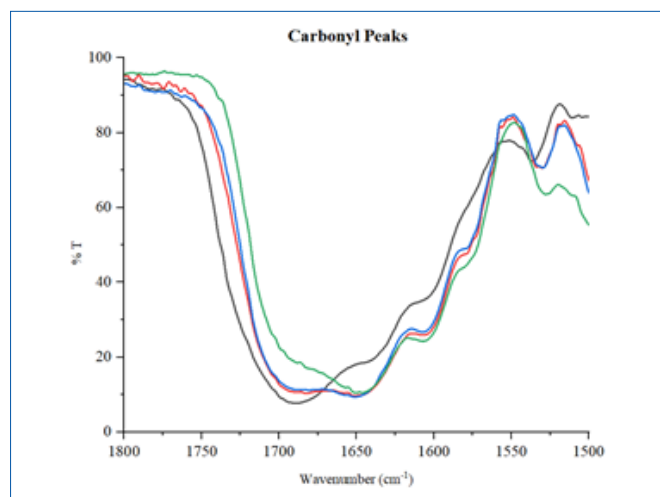


Figure 5: Carbonyl peak of RNA: NaCl formulations at ratio 1:1 at different pre-lyophilization pH - (i) Black - pH 3 (ii) Red - pH 5 (iii) Blue - pH 6 (iv) Green - pH 9.5.

Post-processing of the spectra using software provided with the instrument allowed deconvolution of the carbonyl band (Fig. 6). With deconvolution, four peaks were resolved (1694 , 1646 , 1602 and 1575 cm^{-1}) (Fig. 6) and may represent C=O in the different nucleobases or in different solid environments.^{3,4} However, this region is also susceptible to variable contributions to atmospheric water vapor absorption, which can lead to an increase in noise. These might affect spectral deconvolution results and therefore care must be taken during peak assignment.

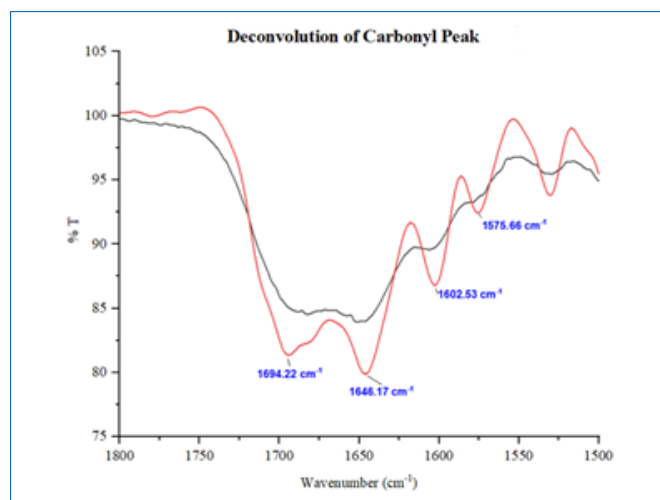


Figure 6: Deconvolution of carbonyl band of RNA: NaCl 1:1 formulation at pH 5. The raw spectrum was deconvoluted using a gamma value of 5 and Bessel smoothing filter with smoothing length of 85% to reduce noise. (i) Black - Original FTIR band (ii) Red - Deconvoluted band.

Discussion and Conclusion

The data from the study points to the effects of the cationic lipids, sucrose and sodium chloride on RNA upon lyophilization to solid state, which is critical to the stability of the active nucleic acid in vaccines and other therapeutic modalities. The IR spectra of the formulations studied show that ionizable excipients interact with the negatively charged phosphate group of RNA, which is an important first step toward the understanding of mRNA stability as phosphodiester bond cleavage plays a key role in the chemical degradation of mRNA.⁶

This study demonstrates the importance of using FTIR technology, in this case PerkinElmer's Spectrum Two FTIR Spectrometer to analyze RNA-excipient interactions in solid samples via assignment of IR active bands to the functional groups present in solid-state formulations of RNA. Hence, we show the feasibility and technical merit of using FTIR method for future evaluations of the structure and stability of RNA in the solid state and its potential on developing solid mRNA formulations.

References

1. Zhao, P. et al. (2020) 'Long-term storage of lipid-like nanoparticles for mRNA delivery', *Bioactive Materials*. Elsevier, 5(2), pp. 358–363. doi: 10.1016/j.bioactmat.2020.03.001.
2. Schoenmaker, L. et al. (2021) 'mRNA-lipid nanoparticle COVID-19 vaccines: Structure and stability', *International Journal of Pharmaceutics*. 2021/04/09. The Author(s). Published by Elsevier B.V., 601, p. 120586. doi: 10.1016/j.ijpharm.2021.120586.
3. Banyay, M., Sarkar, M. and Gräslund, A. (2003) 'A library of IR bands of nucleic acids in solution', *Biophysical Chemistry*, 104(2), pp. 477–488. doi: 10.1016/S0301-4622(03)00035-8.
4. Geinguenaud, F., Militello, V. and Arluison, V. (2020) 'Application of FTIR Spectroscopy to Analyze RNA Structure', in Arluison, V. and Wien, F. (eds) *RNA Spectroscopy: Methods and Protocols*. New York, NY: Springer US, pp. 119–133. doi: 10.1007/978-1-0716-0278-2_10.
5. Kölkenbeck, K. and Zundel, G. (1975) 'The significance of the 2' OH group and the influence of cations on the secondary structure of the RNA backbone', *Biophysics of Structure and Mechanism*, 1(3), pp. 203–219. doi: 10.1007/BF00535757.
6. Mikkola, S., Lönnberg, T. and Lönnberg, H. (2018) 'Phosphodiester models for cleavage of nucleic acids', *Beilstein Journal of Organic Chemistry*, 14, pp. 803–837. doi: 10.3762/bjoc.14.68.

For more information please visit
www.moreinfohere.com